Supporting Information to

In situ construction of built-in electric field for efficient CO_2 electroreduction

Zikang Qiao,[a,] Xiang Han,[a] Tingjie Mao,[a] Zhenrui Yang,[a] Jinglian Huang,[a] Shun Wang,[a] Ping Yu,[b,*] Juan Wang,[a,*] and Huile Jin,[a,*]

[a]Wenzhou Key Lab of Advanced Energy Storage and Conversion, Zhejiang Province Key Lab of Leather Engineering, College of Chemistry and Materials Engineering, Wenzhou University, Wenzhou, Zhejiang 325035, China
[b]Technological Institute of Materials & Energy Science (TIMES), Xi'an Key Laboratory of Advanced Photo-electronics Materials and Energy Conversion Device, Xijing University, Xi'an, 710123, China
*Corresponding author: yupingtina1128@126.com
Juan Wang: juanwang@wzu.edu.cn
Huile Jin: huilejin@wzu.edu.cn

Experimental Procedures

1. Chemicals

For the preparation of materials, indium oxide (In_2O_3, 99.99%), copper nitrate trihydrate ($Cu(NO_3)_2$ $3H_2O$, 99%) were purchased from Shanghai Aladdin Biochemical Technology Co., Ltd, Isopropyl alcohol (C_3H_8O) and polyvinylpyrrolidone (PVP, $(C_6H_9NO)n$, Purity, 1300000) were purchased from Merrell Experimental Equipment (Shanghai) Co., Ltd. Potassium bicarbonate ($KHCO_3$, 99.5%) was purchased from Sinopharm Chemical Reagent Co., Ltd.). Nafion solution (5 wt%, D-520) were used to prepare the catalyst ink. Deionized water was used in this study.

2. Synthesis of CuO/In_2O_3 NPs

Here, the CuO/In_2O_3 NPs was made by mixing different amounts of $Cu(NO_3)_2$ and In_2O_3, and PVP was added to make the two metals uniformly adhere. The fully stirred solution was placed in a quartz boat, and then it was placed in a tubular furnace with a heating rate of 5 degrees per minute from room temperature to 700 ^oC, kept in air for 2 h, and collected into fine powder after dropping to room temperature.

CuO/In_2O_3 NPs (4 mg) was dispersed in isopropanol solution (400 µL), then add the Nafion solution (12 µL), the ink was uniformly dispersed by ultrasound for 30 minutes. The ink (300 µL) was evenly applied onto the gas diffusion layer by a pipette (with a load of 3 mg/cm^2), and dried naturally in an air atmosphere.

3. Characterization

The German Bruker (D8 ADCANCE) X-ray two-dimensional diffractometer was used to collect in situ XRD spectra. Scanning electron microscopy (SEM) imaging was performed on NovaSEM. Transmission electron microscopy (TEM), energy dispersive X-ray spectroscopy (EDS), and high magnification HAADF-STEM were all obtained by FEI talos f200s 200kV field emission transmission electron microscopy and integrated energy spectrometer system Super FEI-X system. Faraday efficiency at different potential was calculated as follows: $FE= z\times F\times n/It$.

4.Electrochemical measurements

The H-type electrolytic cell was consisted of a closed cathode chamber and an anode chamber, separated by the proton exchange membrane in the middle. The three electrodes are assembled with Ag/AgCl (reference electrode), the working electrode, and Pt counter electrode. 99.999% high-purity CO_2 was introduced from the cathode device and the flow rate was set to 20 sccm. Before electrolysis, gas was introduced for 20 minutes to ensure a gas environment for pure CO_2. The liquid was stirred at a constant speed of 280 rpm, resulting in a basically consistent pH of the liquid. The catalyst electrode was placed in a 0.1 M $KHCO_3$ cathode liquid and subjected to pre-treatment with CV scanning for pre catalytic activation, with an activation range of -0.2 to-1.4 V (vs. RHE). Each the same voltage was set to 3600s. After each catalysis, the liquid products were collected and the solution was replaced. The residual gas products were needed to empty in the GC for baseline correction. During the experiment, Shanghai Chenhua CHI760 voltage was applied. The gas-phase products were analyzed using a gas chromatograph (ShimadzuGC-2014). The experiment results were obtained through 500M nuclear magnetic resonance after the suppression of the water peak in liquid product detection.

5. Computational Details

All first-principles calculations were performed using the Vienna Ab initio Simulation Package (VASP). An energy cutoff of 400 eV was applied to the plane-wave basis set, and the k-point sampling was conducted using the Monkhorst-Pack scheme with a (3 × 2 × 1) mesh for optimization purposes. The convergence tolerance of energy and force were set to 10^{-5} eV and 0.02 eV/Å, The computational hydrogen electrode model was employed to evaluate the free energy changes associated with the hydrogen evolution reaction (HER) and carbon dioxide reduction reaction (CO_2RR).

Results and Discussion

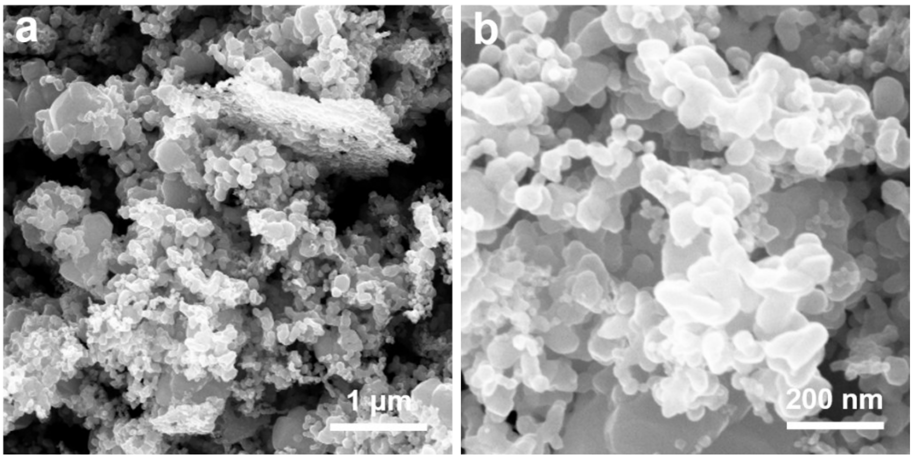

Supplementary Fig. 1 (a, b) SEM images of CuO/In_2O_3 NPs.

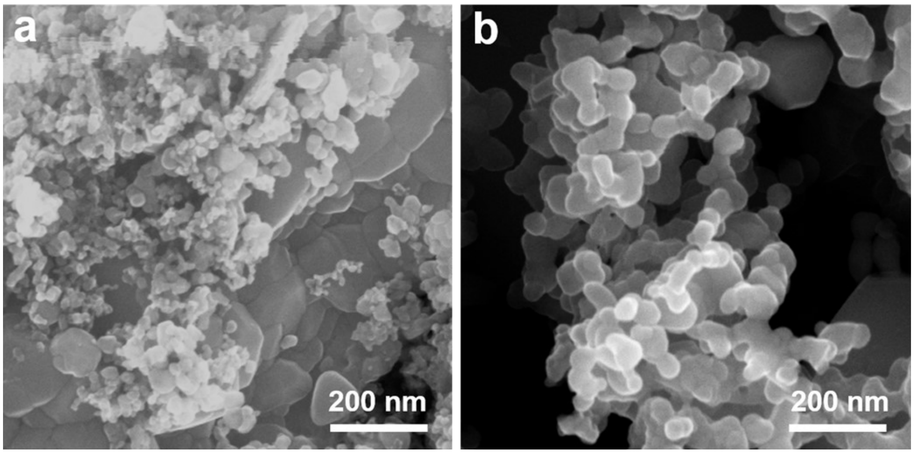

Supplementary Fig. 2 SEM images of CuO/In_2O_3 NPs annealed at (a) 600 ^oC and (b) 800 ^oC.

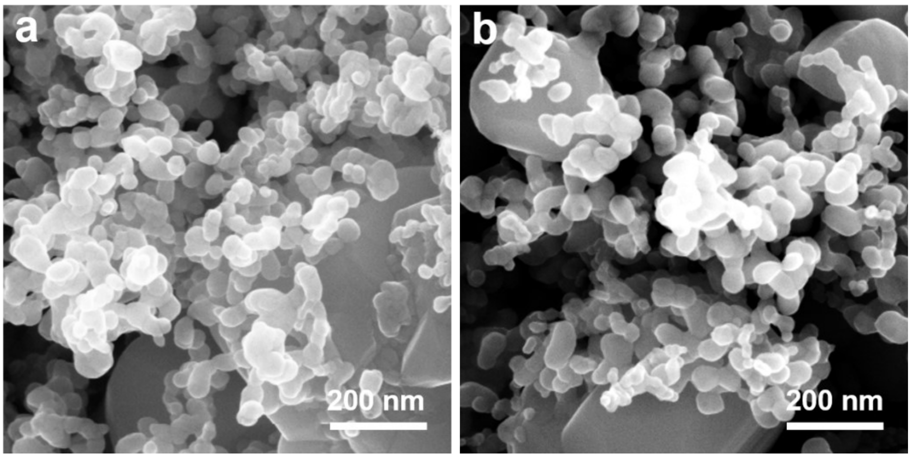

Supplementary Fig. 3 SEM images of CuO/In_2O_3 NPs annealed at 700 °C for (a) 1 h and (b) 3 h.

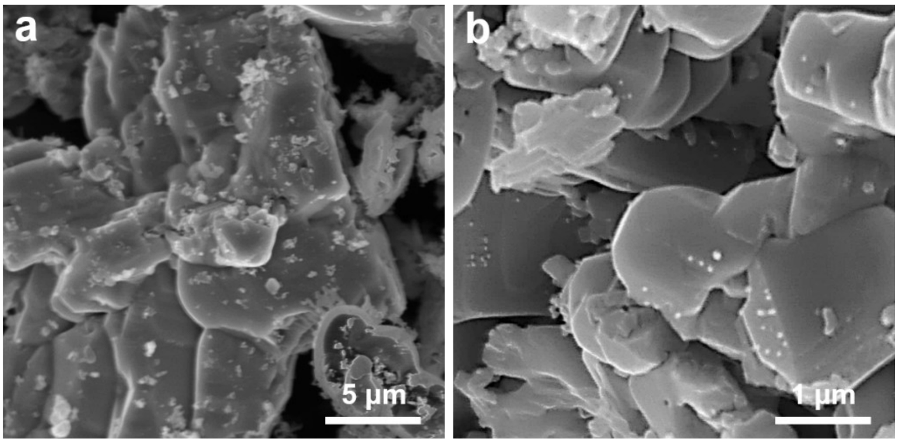

Supplementary Fig. 4 (a, b) SEM images of CuO NPs.

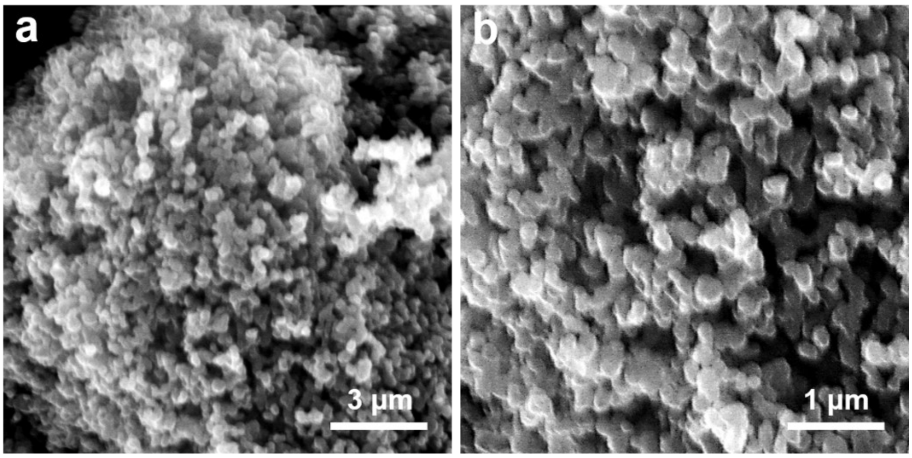

Supplementary Fig. 5 (a, b) SEM images of In_2O_3 NPs.

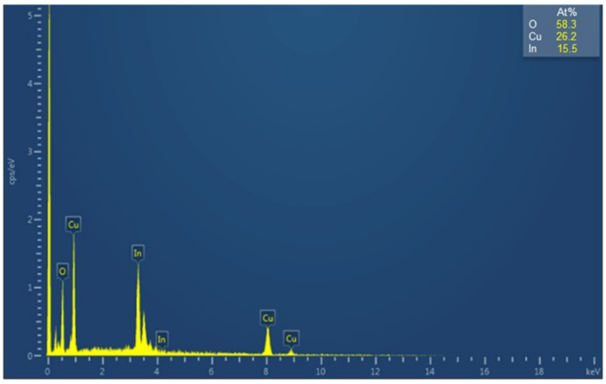

Supplementary Fig. 6 EDS spectrum of CuO/In_2O_3 NPs.

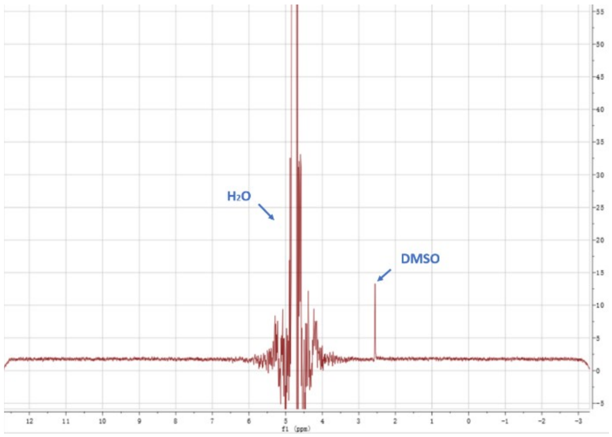

Supplementary Fig. 7 ^{1}H nuclear magnetic spectrum of cathode liquid.

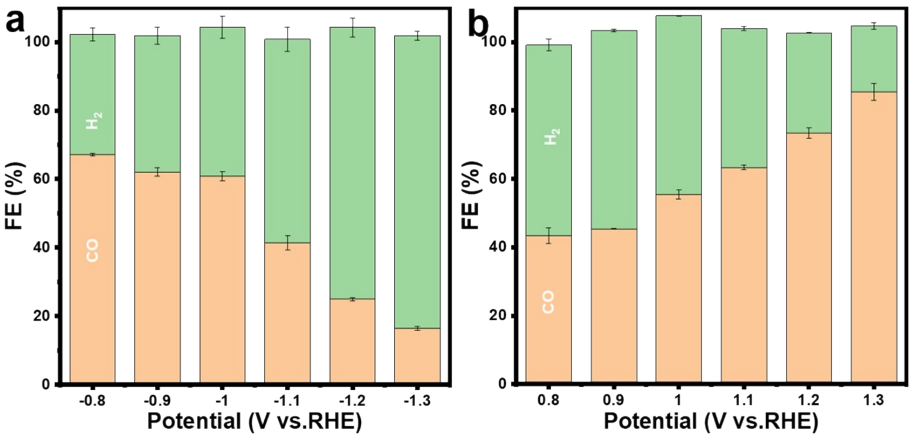

Supplementary Fig. 8 FEs on CuO/In_2O_3 NPs with different Cu/In ratios: (a) 1:1 and (b) 1:2.

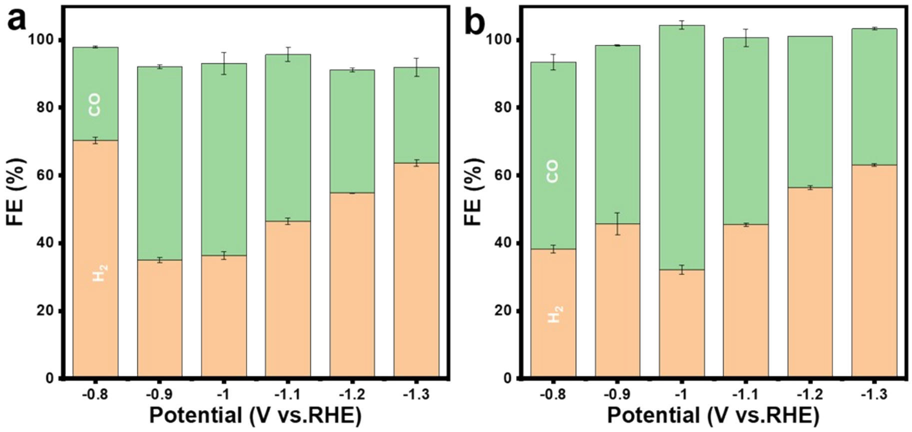

Supplementary Fig. 9 FEs on CuO/In_2O_3 NPs annealed at 700 ^oC for (a) 1 h and (b) 3 h.

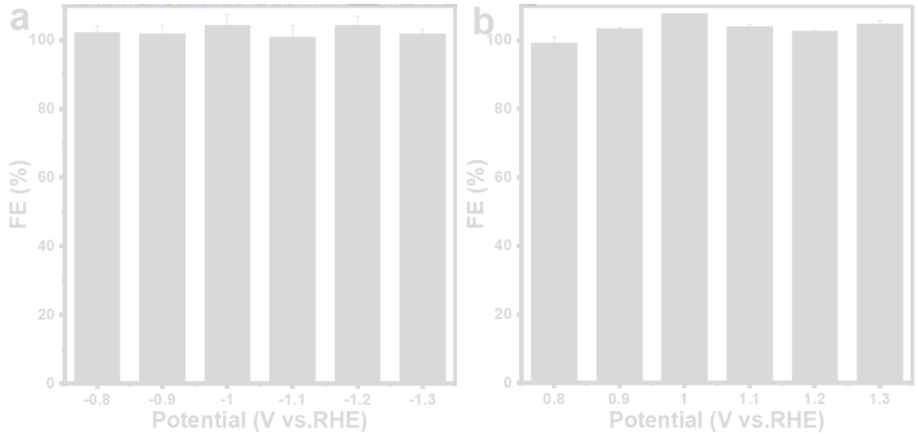

Supplementary Fig. 10 FEs on CuO/In_2O_3 NPs calcined at (a) 600 ^oC and (b) 800 ^oC.

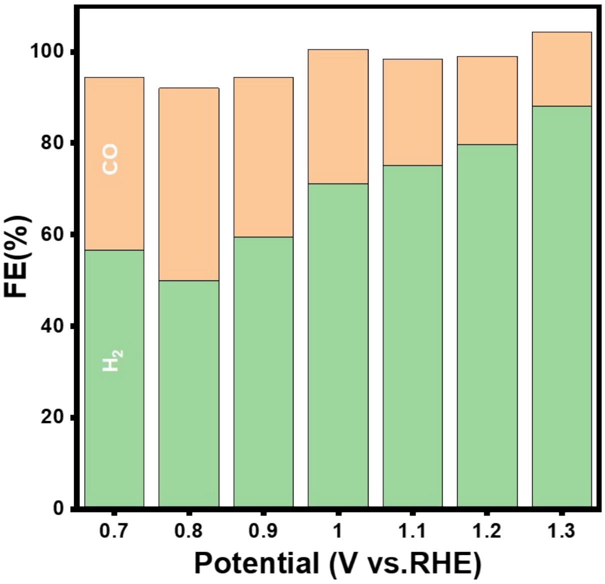

Supplementary Fig. 11. FE on In_2O_3 NPs at various potentials.

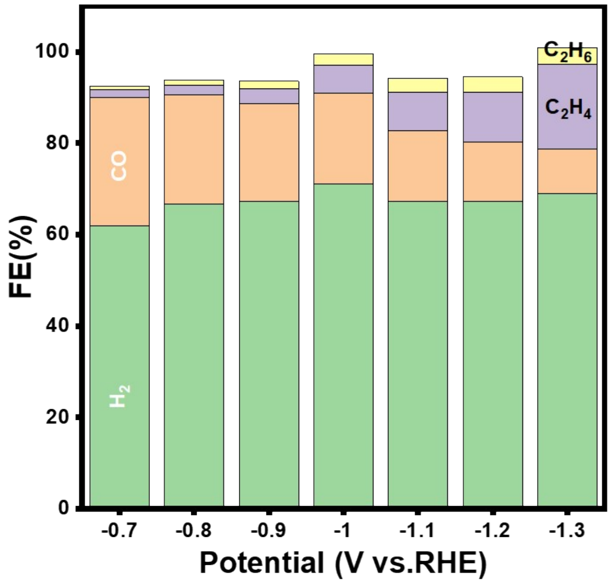

Supplementary Fig. 12. FE on CuO NPs at various potentials.

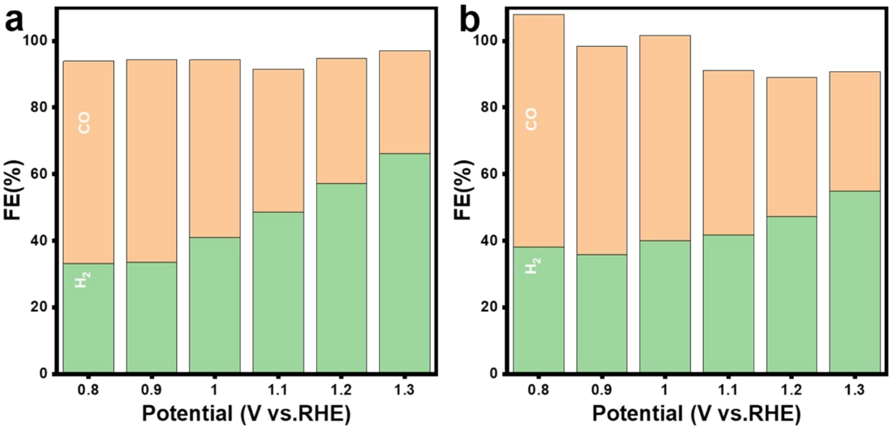

Supplementary Fig. 13. FEs on CuO/In_2O_3 NPs with different PVP quality: (a) 0.1 g and (b) 1.0 g.

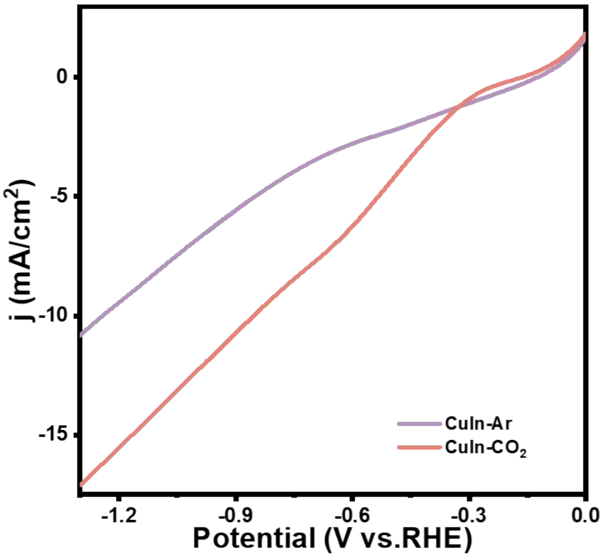

Supplementary Fig. 14. Linear sweep voltammetry of CuO/In_2O_3 NPs under CO_2 and inert conditions.

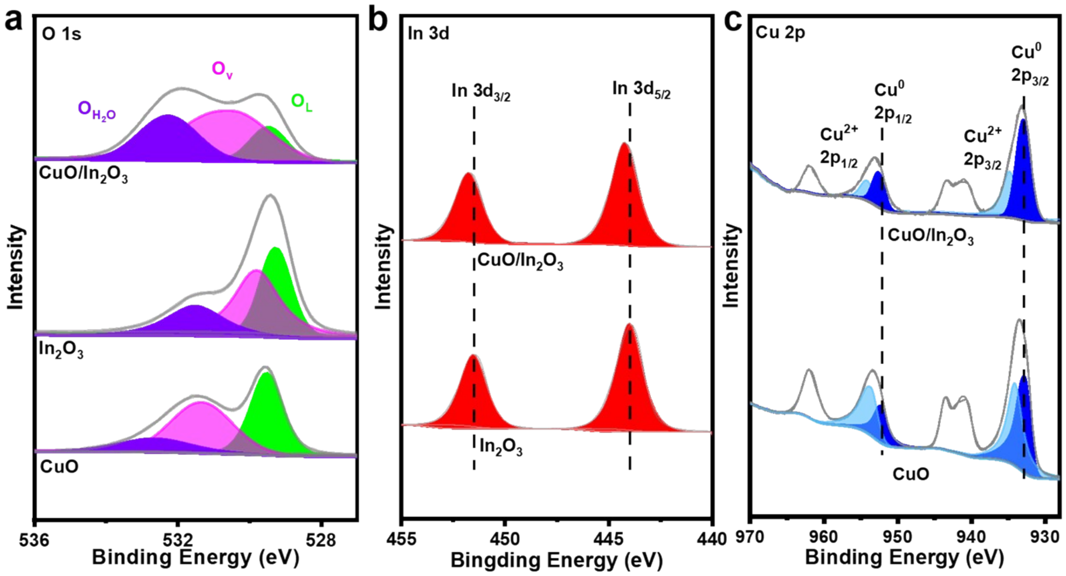

Supplementary Fig. 15. (a) O 1s, (b) In 3d, and (c) Cu 2p XPS spectra of different catalysts.

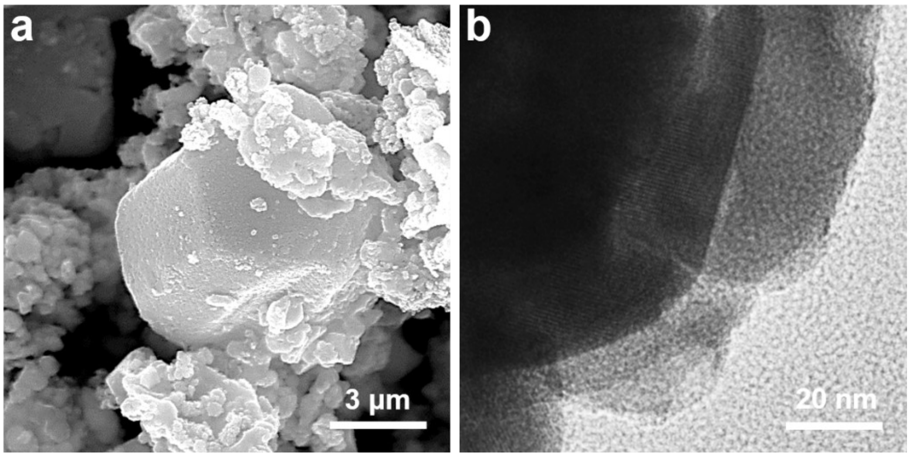

Supplementary Fig. 16. (a) SEM and (b) TEM images of CuO/In_2O_3 after stability test.

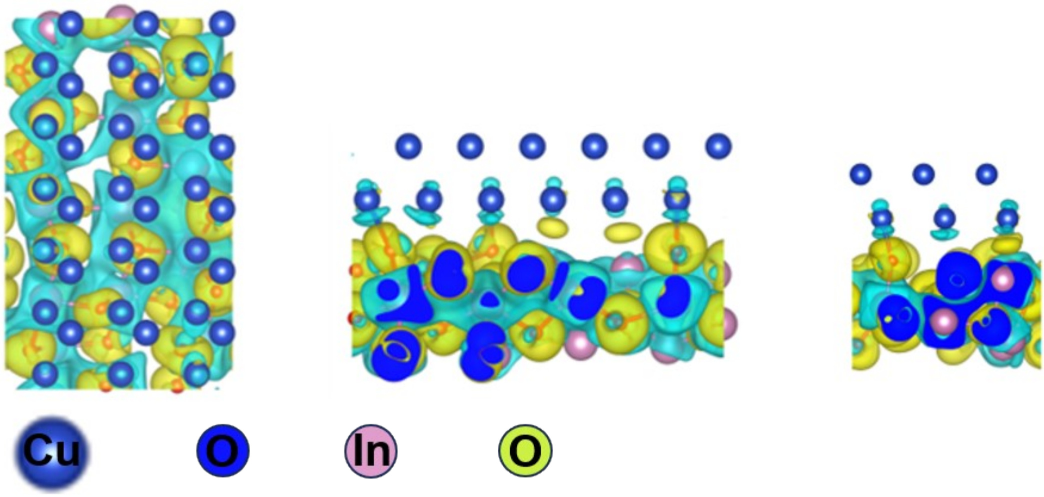

Supplementary Fig. 17. The differential charge distributions for three-dimensional structure. For differential charge distribution diagram, deep blue spheres represent Cu atoms, blue and yellow spheres represent O atoms, and red spheres represent In atoms.

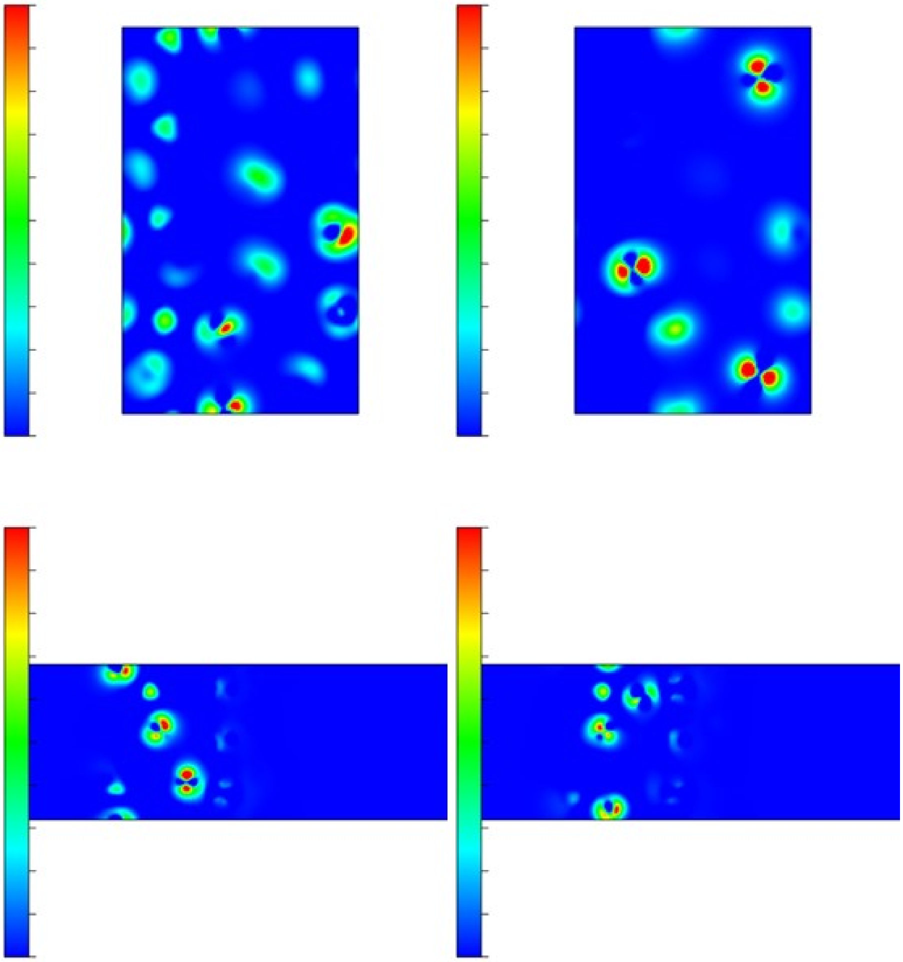

Supplementary Fig. 18. The differential charge distributions for two-dimensional structure. The color scale represents the relative change in electron density, with negative values (blue) corresponding to electron depletion and positive values (red) corresponding to electron accumulation.